Journal of
Composites Science

Article

Examining Mechanical Property Differences in Concrete with Natural and Synthetic Fiber Additives

Walid Fouad Edris [1,2], Samy Elbialy [1,3], Ayman El-Zohairy [4,*], Ashraf Mohamed Soliman [5,6], Shymaa M. M. Shawky [7], Tarek Ibrahim Selouma [2] and Abd Al-Kader A. Al Sayed [7]

[1] Department of Civil and Environmental Engineering, College of Engineering &Design, Kingdom University, Riffa 40434, Bahrain; w.edris@ku.edu.bh (W.F.E.); s.bialy@ku.edu.bh (S.E.)
[2] Department of Civil Engineering, Giza High Institute of Engineering and Technology, Giza 12611, Egypt; tarek_sloma@hotmail.com
[3] Faculty of Engineering in El-Mataria, Helwan University, Cairo 12612, Egypt
[4] Department of Engineering and Technology, Texas A&M University-Commerce, Commerce, TX 75429, USA
[5] Department of Architectural Engineering, College of Engineering & Design, Kingdom University, Riffa 40434, Bahrain
[6] Faculty of Engineering, Minia University, Minia 61111, Egypt
[7] Department of Civil Engineering, Higher Technological Institute, 10th of Ramadan City 44629, Egypt; shymaa.mukhtar@hti.edu.eg (S.M.M.S.); ahmedabdelkader10986@gmail.com (A.A.-K.A.A.S.)
* Correspondence: ayman.elzohairy@tamuc.edu; Tel.: +1-903-468-8683

Abstract: The rapid growth of Natural Fiber Laminate (NFL) innovation is a direct response to environmental challenges, positioning these materials as superior alternatives to synthetic fiber composites. This paper delved into the outcomes of an extensive experimental study investigating the influence of sisal fiber (SLF), banana fiber (BF), and glass fiber (GF) on the mechanical and microstructural characteristics of concrete. The water absorption curves were established for sisal fiber concrete (SLFC), banana fiber concrete (BFC), and glass fiber concrete (GFC). Furthermore, Scanning Electron Microscope (SEM) observations were conducted to perform microanalysis and failure analysis of the tested specimens. The results revealed significant improvements in the concrete containing fibers compared to its counterpart in fiber-free concrete. For mixtures with a water-to-binder (W/B) ratio of 0.3, the most optimal mix (GF-30-135) showed improvements in compressive strength, flexural strength, and splitting tensile strengths by 4.13%, 8.93%, and 10.10%, respectively. On the other hand, for W/B of 0.4, mix GF-30-135 showed improvements of 5.05%, 8.55%, and 11.60%, respectively. Furthermore, as the fiber content increased, microscopic analyses revealed a weakening of the bond between the fibers and the rest of the matrix, contributing to the deterioration of the mechanical properties.

Keywords: natural fibers; synthetic fibers; sisal fibers; banana fibers; glass fibers; mechanical properties; scanning electron microscope; concrete

check for updates

Citation: Edris, W.F.; Elbialy, S.; El-Zohairy, A.; Soliman, A.M.; Shawky, S.M.M.; Selouma, T.I.; Al Sayed, A.A.-K.A. Examining Mechanical Property Differences in Concrete with Natural and Synthetic Fiber Additives. *J. Compos. Sci.* **2024**, *8*, 167. https://doi.org/10.3390/jcs8050167

Academic Editor: Francesco Tornabene

Received: 14 March 2024
Revised: 15 April 2024
Accepted: 22 April 2024
Published: 30 April 2024

1. Introduction

The widespread application of concrete in construction can be attributed to its manifold advantages, encompassing high mechanical strength, ease of production and shaping, and comparatively economical costs [1–5]. However, concrete is often characterized as a brittle material with limited deformability and a tendency to rapidly propagate cracks under tensile stresses. In light of this, the incorporation of dispersed fibers into the cementitious matrix emerges as a viable alternative to mitigate this constraint [4]. These fibers act as bridges in areas prone to cracking, effectively transferring stresses and augmenting the effectiveness of fiber-reinforced concrete following the initiation of cracks [4,6,7]. As a result, there is an increased capacity for energy absorption and a reduction in the propagation and expansion of the existing cracks [8,9]. Fibers are traditionally reinforced materials, with a history of serving various practical purposes [1,10,11]. These fibers comprise both natural and synthetic types. Synthetic fibers include materials such as asbestos, carbon, glass, and engineered substances. On the other hand, natural fibers encompass sisal, jute, horsehair, banana, glass, bamboo, coconut strands, elephant grass, and others [1,3,12]. The application of these materials to utilize natural fibers as reinforcement in concrete is a relatively recent development [1,13]. The unique attributes of natural fiber-reinforced concrete encompass enhancements in flexural strength, tensile strength, durability, and impact resistance [1]. Strength in this context pertains to their ability to withstand deterioration caused by external and internal factors.

Natural fibers, such as sisal, are abundant in tropical regions, placing them within the sustainable materials category [3]. Certain natural fibers exhibit tensile strengths surpassing those of polypropylene (PP) fibers and comparable to polyvinyl acetate (PVA) fibers, providing performance akin to composites crafted from synthetic or steel fibers [3]. Sisal fiber, derived from the Agave Sisalana plant and recognized as one of the most extensively researched natural fibers for cement-based composites, distinguishes itself through widespread availability and exceptional mechanical properties. This makes it a prime choice among available natural fibers for applications in the construction industry [5,12]. Sisal fiber stands out not only for its cost-effectiveness but also for its elevated tensile strength, abrasion resistance, and toughness. Additionally, it poses no health-related risks and offers favorable thermal and acoustic properties [3,14]. A thorough experimental program was undertaken to examine the mechanical performance of masonry hollow blocks manufactured using a combination of concrete and natural sisal fibers [14]. Interestingly, the inclusion of sisal fibers in the concrete mixture did not lead to an enhancement in the individual blocks' mechanical properties, specifically in terms of compressive strength and elastic modulus [14]. However, a notable positive effect was observed in the ductility of the blocks. The fibers played a crucial role in bridging the sides of opening cracks, effectively resisting the loss of material continuity [15].

Banana plantations are widespread worldwide, with over 300 species belonging to the Musaceae family [16]. Banana trees are commonly found in regions with a warm climate. In recent times, there has been a growing interest in both water hyacinth and banana fibers [17,18]. In a general sense, both water hyacinth fiber and banana fiber, extracted from the banana plant, share a common composition characterized by hollow cellulose fibrils interwoven within a matrix of lignin, cellulose, and hemicellulose [19]. Cellulose and hemicellulose influence the tensile strength and moisture absorption properties of these materials, whereas lignin contributes to their resistance against biodegradation [20]. Moreover, the microstructures and inherent traits of plant fibers, including thickness, density, porosity, rigidity, resistance, conductivity, and air permeability, are instrumental in shaping their mechanical and thermal properties. The introduction of banana fibers represents an innovative enhancement to construction materials. The incorporation of banana fibers into the concrete mix design aims to substantially augment the internal strength of concrete [18]. Dhawan et al. [21] explored the utilization of sisal and banana fibers to enhance the strength and applications of concrete. The research findings indicated that incorporating banana fiber led to an enhancement in the concrete's crack resistance and resistance to spalling. According to Naaamandadin et al. [22], the inclusion of banana fiber contributes to the enhancement of concrete's flexural strength due to its favorable mechanical properties.

The integration of glass fibers (GF) into concrete is a commonly employed method to improve the mechanical properties and longevity of the composite material. Crafted from strands of molten glass, glass fibers are typically dispersed throughout the concrete mix to establish a reinforced framework. Serving as secondary reinforcement, these fibers enhance the concrete's tensile strength, impact resistance, and flexural performance [23]. The incorporation of GF also helps mitigate cracking and improve the overall ductility of the material [24]. Choi and Yuan [25] attained reductions in the concrete's compressive strength after incorporating GF in concrete. However, an increase in the concrete's splitting tensile strength and enhancement in its ductility were obtained. Khan and Ali [24] and Kizilkanat et al. [26] reported improvements in the concrete's compressive strength, splitting tensile strength, flexural strength, and fracture energy after adding GF to concrete. However, reductions in the concrete's compressive strength were found [27].

The application of Natural Fiber Laminate (NFL) to concrete is a relatively recent development. The benefits of these innovative materials over others, like synthetic fiber composites, are in need of further investigation. Hence, this research work comprehensively illustrates the results of experimental investigations delving into the influence of sisal fiber (SLF), banana fiber (BF), and glass fiber (GF) on both the mechanical and microstructural characteristics of concrete. Various concrete specimens were carefully prepared, each incorporating different water-to-binder (W/B) ratios, fiber contents, and curing durations. Subsequent testing of these specimens was carried out to collect data on their mechanical properties. Furthermore, Scanning Electron Microscope (SEM) observations were performed to facilitate microanalysis and failure analysis of the tested specimens.

2. Experimental Program

2.1. Materials

2.1.1. Cement and Admixtures

We utilized Ordinary Portland Cement (OPC) type I [42.5 N] in the concrete blends, under cutting-edge practices in the construction industry and adherence to both the Egyptian ES 4756/1-2013 [28] and European EN 197/1-2011 [29] standards. For the promotion of homogeneity within the concrete mixtures, we introduced Sika Visco-Crete 3425 admixture [30]. This admixture, characterized by a specific gravity of 1.08 and a 2% cement content, aligns with the specifications outlined in ASTM C494/C494M-19 [31]. The chemical compositions of the OPC are detailed in Table 1.

Table 1. Chemical compositions of OPC.

Cement	SiO_2	Al_2O_3	Fe_2O_3	CaO	MgO	SO_3	K_2O	Na_2O	LOI *
I 42.5N	21.3	4.7	3.9	63.7	1.8	2.5	0.48	0.18	3.1

* LOI: Loss of ignition.

2.1.2. Aggregates

We utilized coarse aggregate (CA), consisting of naturally crushed dolomite with a nominal maximum size of 19 mm, and fine aggregate (FA), comprising natural sand characterized by a specific gravity of 2.58. The fine aggregate exhibited a size distribution ranging from 0.15 to 1.2 mm, forming the components for the preparation of the concrete mixes. The used aggregates comply with ASTM C33/C33M-08 [32]. The grading size distributions of these aggregates are illustrated in Figure 1. Furthermore, Table 2 presents an overview of the physical and mechanical properties.

Table 2. The physical and mechanical properties of the coarse and fine aggregates.

Property	Coarse Aggregate	Fine Aggregate
Specific gravity	2.6	2.5
Volume density (Kg/m^3)	1430	1612
Water absorption %	0.8	1.9
Los Angeles abrasion %	17.5	-
Crushing value %	17.9	-

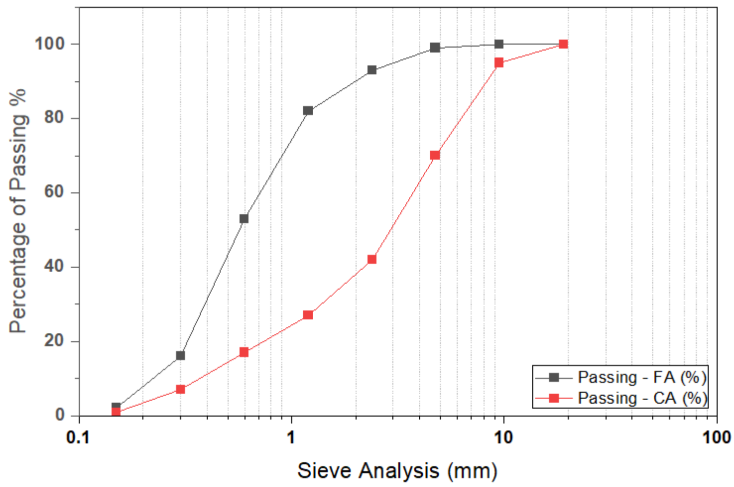

Figure 1. Particle size distributions of the coarse and fine aggregates.

2.1.3. Properties of Fibers

The sisal fibers employed in this study originated from Kafr El Dawar city, located in the Beheira Governorate of Egypt. These fibers were extracted from the Agave sisalana plant using a decortication process, and they were acquired in bundles of long fibers, each measuring approximately 1000 mm in length. The fibers were processed to eliminate impurities and then were immersed in water at a temperature of 70 ± 5 °C for one hour. Following this treatment, the fibers were air-dried for 48 h and then manually cut to the desired length (35 mm). The natural white appearance of sisal fibers is depicted in Figure 2a.

(**a**) Sisal fibers (SLF) (**b**) Banana fibers (BF) (**c**) Glass fibers (GF)

Figure 2. The different fibers used in this study.

The banana pseudo-stem was obtained from the banana plant segment which resembles a trunk with a soft central core and tightly wrapped by up to 25 leaf sheaths and classified as leaf fiber of natural vegetable fiber according to ASTM D123-52 [33]. It was supplied by Papyrus Egypt [34] (Nubaria Region, Egypt). Figure 2b shows the natural light-brown banana fibers. The fibers were extracted from the banana pseudo-stem leaves using a decorticator machine immediately after the pseudo-leaves' stems were cut. The extraction procedures were initiated with the first stage, known as tuxing, which involves separating fiber bundles from the remaining pieces. Following that, the second phase involved removing non-fibrous parts and any residual components in the fibers.

The glass fiber (as depicted in Figure 2c) was sourced from the Egyptian European Steel Fiber company (Nasr City, Egypt). The mechanical, physical, and chemical properties of the used fibers (SLF, BF, and GF) are listed in Table 3. Noteworthy properties include isotropy, affordability, easy availability, and excellent chemical resistance. All fibers had the same length of 35 mm. Moreover, Figure 3 illustrates the typical cross-sectional areas captured through scanning electron microscopy (SEM) and the essential elements identified through EDAX spectrum analysis using spot scan EDAX of the used fibers.

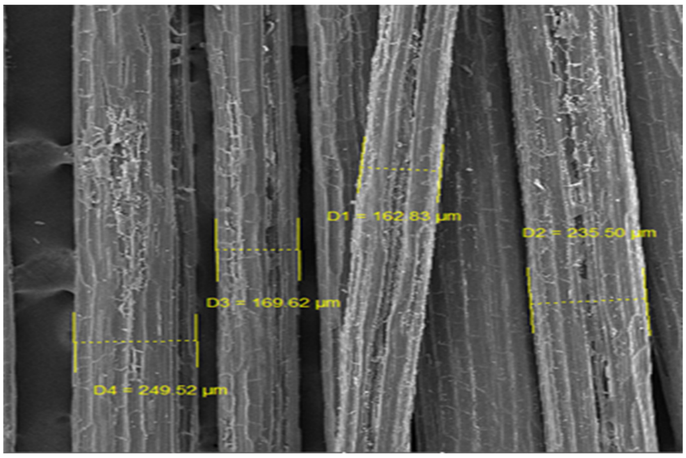

(**a**) SEM of sisal fibers (SLF) – magnification × 100

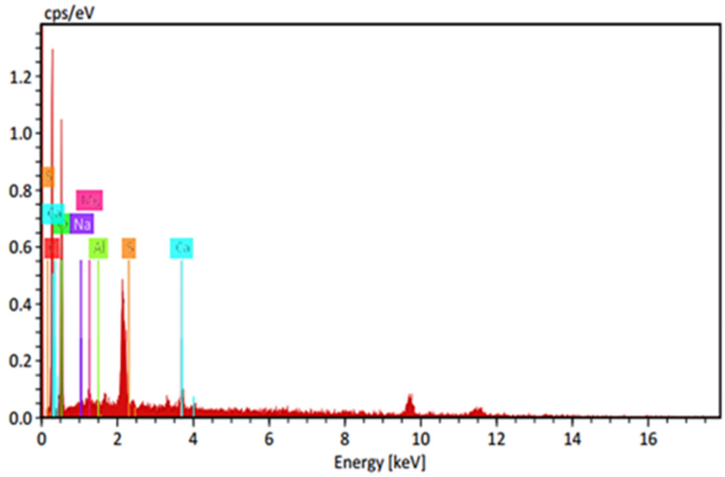

(**b**) EDAX spectrum analysis image of sisal fibers (SLF)

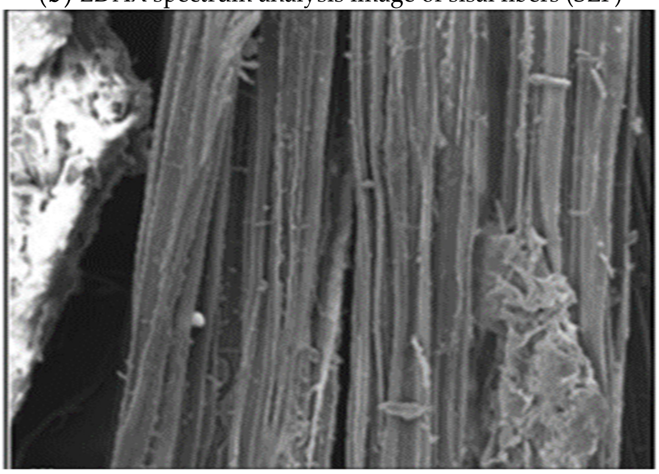

(**c**) SEM of banana fibers (BF) - magnification × 244

Figure 3. *Cont.*

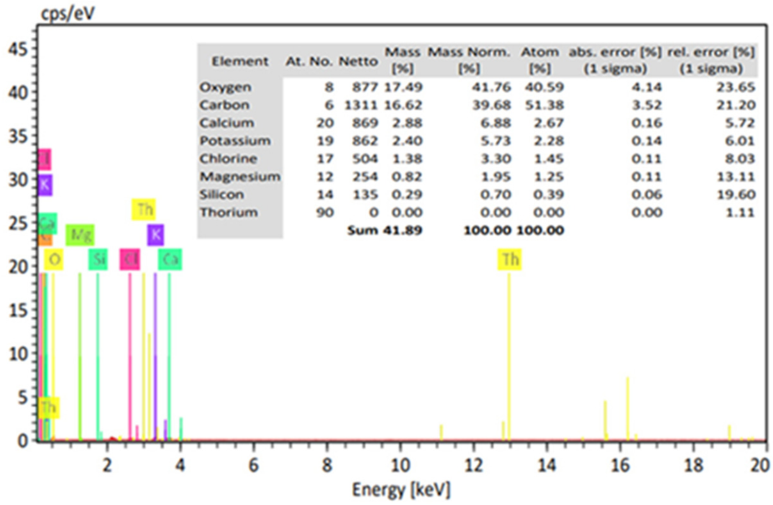

Element	At. No.	Netto	Mass [%]	Mass Norm. [%]	Atom [%]	abs. error [%] (1 sigma)	rel. error [%] (1 sigma)
Oxygen	8	877	17.49	41.76	40.59	4.14	23.65
Carbon	6	1311	16.62	39.68	51.38	3.52	21.20
Calcium	20	869	2.88	6.88	2.67	0.16	5.72
Potassium	19	862	2.40	5.73	2.28	0.14	6.01
Chlorine	17	504	1.38	3.30	1.45	0.11	8.03
Magnesium	12	254	0.82	1.95	1.25	0.11	13.11
Silicon	14	135	0.29	0.70	0.39	0.06	19.60
Thorium	90	0	0.00	0.00	0.00	0.00	1.11
		Sum	41.89	100.00	100.00		

(**d**) EDAX spectrum analysis image of banana fibers (BF)

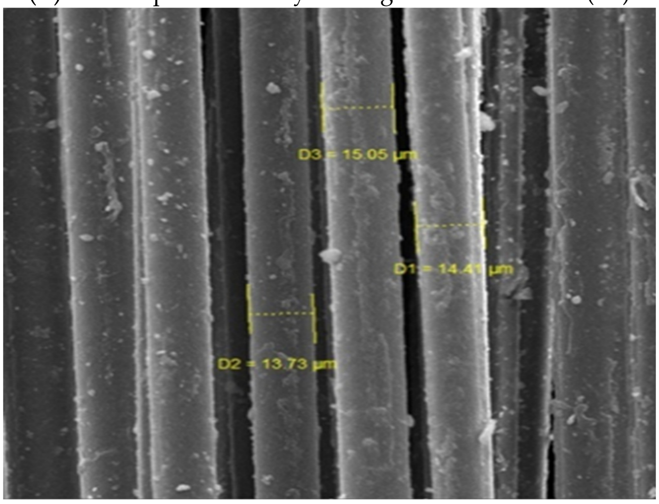

(**e**) SEM of glass fibers (GF) - magnification × 1000

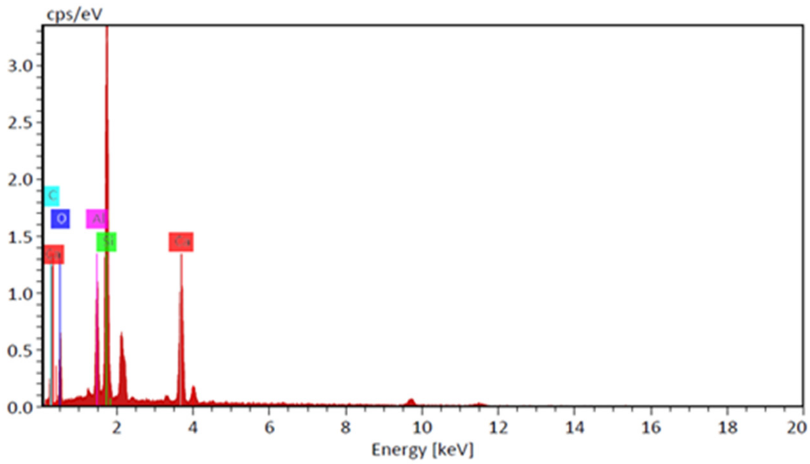

(**f**) EDAX spectrum analysis image of glass fibers (GF)

Figure 3. SEM and EDAX spectrum analysis images for all sisal fibers (SLF), banana fibers (BF), and glass fibers (GF).

Table 3. Mechanical, physical, and chemical properties of fibers.

Fiber Type	Sisal Fiber	Banana Fibers [33]	Glass Fiber
	SLF	**BF**	**GF**
	Mechanical Properties		
Tensile Strength (MPa)	380	754	1755
Young's modulus (GPa)	5.24	27	78.51
Elongation Break (%)	15.9	10.35	17.2
* L/D ratio	160	150	980
	Physical Properties		
Density (Kg/m^3)	1450	1350	2550
Moisture content	10.47	10	0.6
Water absorption (%)	80.5	61.2	38.7
Width or Diameter (µm)	250–650	80–250	13.8
	Chemical Composition (%)		
Cellulose	65	63.2	--
Hemicellulose	12	18.6	--
Waxes	2	0.3	--
Lignin	9.9	5.10	--

* L/D is the ratio of the length to diameter of the fibers.

2.2. Mixture Proportions

Table 4 enumerates the specific concrete blends employed in fabricating the specimens. Various proportions of SLF, BF, and GF (0.45%, 0.9%, and 1.35% by volume) were utilized, along with W/B ratios of 0.3 and 0.4. The concrete formulation adhered to the directives outlined in ACI 211.1-91 [35] and ACI 544.1R-96 2002 [36]. The mixing process began with the addition of raw materials into the forced mixer, following specified stirring durations. This proceeded as follows: the coarse and fine aggregates were introduced into the forced mixer and stirred for approximately 20 s. Cement was introduced and stirred for an additional 20 s. Subsequently, approximately 30% water was introduced and mixed thoroughly for around 90 s. Fiber, combined with 30% water, was introduced, and the mixture was stirred for an additional 90 s. Subsequently, a superplasticizer was added, and the remaining water was introduced, with stirring continuing until a uniform colloid was achieved. In order to achieve the desired slump for fresh concrete, a high-performance water reducer of the polycarboxylate type was utilized. Subsequently, all fiber blends were manually distributed throughout the concrete mixture, and the mixing process continued to ensure complete homogeneity. Distinctive nomenclatures were assigned to each concrete mix, delineating the components within. For instance, in GF-30–45, 'GF' signifies the incorporation of glass fiber, '30' denotes a W/B ratio of 0.30, and '45' indicates a fiber dosage of 0.45%. In parallel, the concrete mix devoid of fibers was denoted as 'PC,' exemplified by 'PC-30', where 'PC' designates the absence of fibers and '30' signifies a W/B ratio of 0.30.

Table 4. Mixture proportions of the concrete mixes.

Mix. ID	W/B	% Fiber by Vol.			Cement	Sand	Coarse agg.	Water	SP
		SLF	**BF**	**GF**	**Kgm^{-3}**	**Kgm^{-3}**	**Kgm^{-3}**	**Kgm^{-3}**	**Kgm^{-3}**
				Phase I—W/B ratio 0.30					
PC-30	0.35	--	--	--	450	800	1145	135	8
SLF-30-45	0.30	0.45	--	--	450	800	1145	135	8
SLF-30-90	0.30	--	0.90		450	800	1145	135	8

Table 4. *Cont.*

Mix. ID	W/B	% Fiber by Vol.			Cement	Sand	Coarse agg.	Water	SP
		SLF	BF	GF	Kgm^{-3}	Kgm^{-3}	Kgm^{-3}	Kgm^{-3}	Kgm^{-3}
SLF-30-135	0.30	--	--	1.35	450	800	1145	135	8
BF-30-45	0.30	0.45	--	--	450	800	1145	135	8
BF-30-90	0.30	--	0.90		450	800	1145	135	8
BF-30-135	0.30	--	--	1.35	450	800	1145	135	8
GF-30-45	0.30	0.45	--	--	450	800	1145	135	8
GF-30-90	0.30	--	0.90	--	450	800	1145	135	8
GF-30-135	0.30	--	--	1.35	450	800	1145	135	8
Phase II—W/B ratio 0.40									
PC-40	0.40	--	--	--	450	750	1080	180	7
SLF-40-45	0.40	0.45	--	--	450	750	1080	180	7
SLF-40-90	0.40	--	0.90		450	750	1080	180	7
SLF-40-135	0.40	--	--	1.35	450	750	1080	180	7
BF-40-45	0.40	0.45	--	--	450	750	1080	180	7
BF-40-90	0.40	--	0.90		450	750	1080	180	7
BF-40-135	0.40	--	--	1.35	450	750	1080	180	7
GF-40-45	0.40	0.45	--	--	450	750	1080	180	7
GF-40-90	0.40	--	0.90	--	450	750	1080	180	7
GF-40-135	0.40	--	--	1.35	450	750	1080	180	7

2.3. Preparation of the Specimens and Test Procedures

A total of 72 cubes, each measuring 100 mm × 100 mm × 100 mm, were utilized to conduct compressive strength tests on the specimens. Moreover, a total of 72 cylinders, each with dimensions of 150 × 300 mm, were employed to assess the splitting tensile strength of the specimens. A set of 42 prisms, each with dimensions of 100 mm × 100 mm × 400 mm, was employed to evaluate the four-point flexural strength of the specimens. Absorption measurements were performed on cubic specimens measuring 100 mm × 100 mm × 100 mm. Table 5 lists the total number of specimens for each test. During the curing process, the concrete specimens were kept in the plastic molds for 24 h. Following the extraction of the specimens, they were submerged in room temperature water until testing ages of either 7 or 28 days.

Table 5. Dimensions and total number of specimens for each test.

Test	Size of Specimens	Fiber Length	Volume % of Fiber	Total Number
Compressive Strength	Cubes 100 × 100 × 100	35 mm length	0.45, 0.9, and 1.35	72
Flexural Strength	Prisms 100 × 100 × 400	35 mm length	0.45, 0.9, and 1.35	72
Splitting tensile strength	Cylinders 150 × 300	35 mm length	0.45, 0.9, and 1.35	72
Absorption %	Cubes 100 × 100 × 100	35 mm length	0.45, 0.9, and 1.35	72
SEM—28 days	20 × 15 × 10	35 mm length	0.45, 0.9, and 1.35	9
Total number of concrete samples				279

Each group underwent testing with three specimens, and the adopted results represent the average. The subsequent investigations were conducted as follows:

2.3.1. Workability

The workability of fresh concrete, indicating its fluidity, was assessed using a 300 mm height slump cone following ASTM C143/C143M-15 [37].

2.3.2. Compressive Strength

Compression testing employed a machine with a maximum capacity of 1500 KN and a loading rate of 0.6 MPa/second. The aim was to assess the strength development in the specimens at various ages. The tests adhered strictly to the guidelines specified in BS 1881-116, ensuring a standardized and precise evaluation of the samples [38]. Compression strength tests were conducted at 7 and 28 days for each blend, with three samples examined for each duration.

2.3.3. Flexural Strength

The concrete prisms underwent testing at both 7 and 28 days in accordance with ASTM C78/C78M-22 [39]. For each mixture, three specimens were tested to assess flexural strength.

2.3.4. Splitting Tensile Strength

Splitting tensile strength was assessed following the guidelines of ASTM C496/C496M-1 [40]. During this test, a compressive force was applied along the length of the cylinders to load the specimens. The tensile strength was determined by dividing the maximum load (2P) sustained by the specimens by the relevant geometric factors (πDL). The reported result represents the average value derived from triplicate specimens.

2.3.5. Water Absorption

Samples measuring 100 mm × 100 mm × 100 mm were retrieved, air-dried at room temperature, and further subjected to drying at 100–110 °C in an oven adhered to the ASTM C642-2013 [41] to perform the water absorption test. The samples were immersed in a water tank with a depth of 20 cm and a temperature ranging from 18 to 20 °C after recording their masses. At the age of 7 days, the samples underwent weighing every 24 h to monitor the deviation in water absorption.

2.3.6. SEM Observation

Following the ASTM C1723-2010 standard [42], the SEM images were taken for the prepared samples. The specimens selected for SEM observation were roughly 20 mm × 15 mm × 10 mm in size, encompassing aggregate, fibers, and the cement matrix simultaneously. Following a gold coating process, these sections were positioned on the SEM scanning table.

3. Results and Discussions

Table 6 lists a summary of the test results. The table provides comprehensive data for each test, encompassing mix designation, density, slump measurement, compressive strength, flexural strength, and tensile strength.

Table 6. Summary of the test results.

Mix Designation	Slump (mm)	Absorption (%)		f'_c (MPa)		f_r (MPa)		f_{spt} (MPa)	
		7 Days	28 Days	7 Days	28 Days	7 Days	28 Days	7 Days	28 Days
Phase I—W/B ratio 0.30									
PC-30	137	2.44	2.46	25.11	40.21	3.58	5.71	2.68	4.06
SLF-30-45	131	2.42	2.45	26.48	40.11	3.66	5.86	2.76	4.24
SLF-30-90	122	2.38	2.48	27.16	40.4	3.68	5.9	2.83	4.29

Table 6. *Cont.*

Mix Designation	Slump (mm)	Absorption (%)		f'_c (MPa)		f_r (MPa)		f_{spt} (MPa)	
		7 Days	28 Days	7 Days	28 Days	7 Days	28 Days	7 Days	28 Days
SLF-30-135	98	2.37	2.53	27.85	40.99	3.78	6.01	2.87	4.32
BF-30-45	123	2.38	2.47	26.87	40.7	3.72	5.95	2.82	4.26
BF-30-90	117	2.36	2.50	27.56	40.89	3.76	5.97	2.89	4.33
BF-30-135	95	2.35	2.54	28.34	41.38	3.78	6.06	2.96	4.38
GF-30-45	136	2.44	2.41	28.54	41.19	3.8	6.05	3.02	4.36
GF-30-90	132	2.45	2.37	29.13	41.87	3.86	6.14	3.06	4.39
GF-30-135	110	2.47	2.31	29.62	40.99	3.91	6.22	3.12	4.47
Phase II—W/B ratio 0.40									
PC-40	158	2.42	2.44	25.5	40.8	3.52	5.85	2.95	4.74
SLF-40-45	147	2.41	2.42	26.87	40.7	3.71	5.97	3.06	4.8
SLF-40-90	140	2.36	2.43	27.56	41.68	3.81	6	3.18	4.85
SLF-40-135	128	2.30	2.47	26.97	41.97	3.93	6.09	3.23	4.91
BF-40-45	141	2.34	2.36	27.26	41.29	3.86	6.03	3.18	4.85
BF-40-90	132	2.27	2.39	27.95	41.87	4.04	6.17	3.3	5.03
BF-40-135	127	2.22	2.51	26.28	42.66	4.19	6.31	3.41	5.09
GF-40-45	154	2.32	2.41	28.93	41.78	4.04	6.17	3.38	5.05
GF-40-90	141	2.21	2.36	29.81	42.86	4.29	6.35	3.54	5.29
GF-40-135	127	2.18	2.31	28.83	41.38	4.14	6.23	3.51	5.27

3.1. Workability

As depicted in Figure 4, the slump test was performed to assess the workability of concrete, both with and without fibers. For the SLF and W/B ratio of 0.3, there were 4.4%, 10.9%, and 28.5% reductions in the slump readings for the fiber contents of 0.45%, 0.9%, and 1.35%, respectively. These reductions became 10.2%, 14.5%, and 30.6% in the case of BF. These reductions increased to 0.7%, 3.6%, and 19.7% when the GF was used. The results in general indicated that workability decreased irrespective of the fiber volume fractions. However, the reduction was enhanced in the cases of SLF and BF relative to the case of GF. It was notable that the use of GF resulted in greater workability. This could be attributed to the water absorption by the fibers [3,16]. The inherent characteristics of SLF and BF as plant fibers with a higher water absorption capacity led to these reductions in workability. Moreover, the used fibers can act as obstacles to the movement of concrete particles, making it more challenging to place and finish the concrete. Irrespective of the fiber volume fractions, there were no signs of fiber agglomeration or heterogeneity in the samples during the mixing process. According to Figure 4, increasing the SLF ratio from 0.45% to 1.35% led to workability reductions of 28.5% and 18.9% for the W/B ratios 0.3 and 0.4, respectively, relative to the control specimen (PC-30). However, these reductions were 30.6% and 19.6% in the case of BF contents. Moreover, including the GF in the concrete mixes caused reductions of 19.7% for the two W/B ratios.

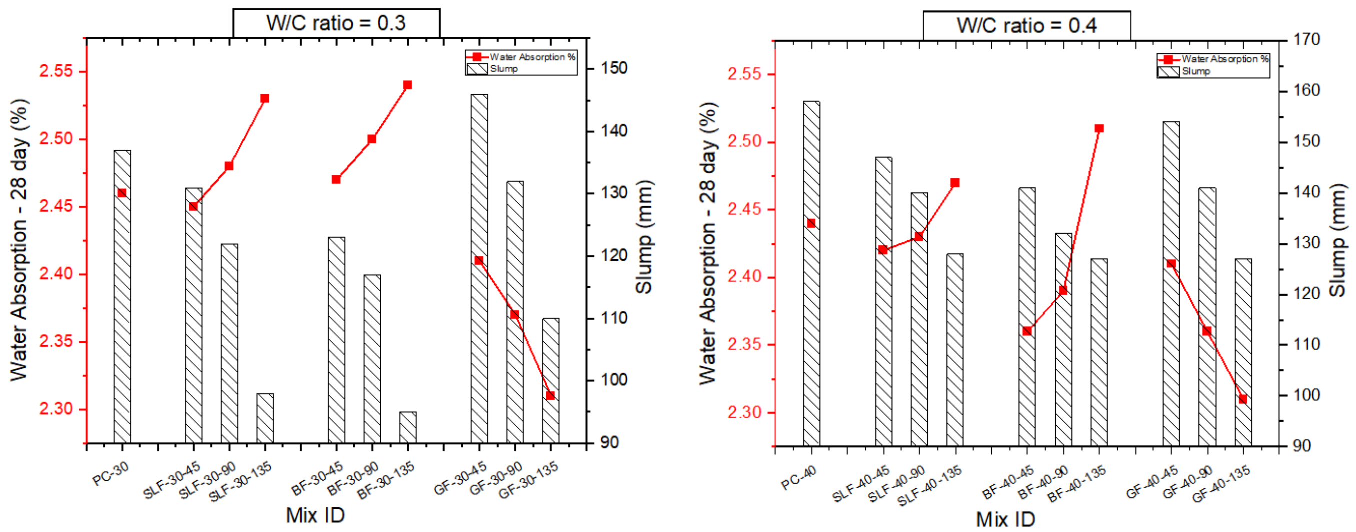

(**a**) For the water/binder ratio of 0.3 (**b**) For the water/binder ratio of 0.4

Figure 4. Slump and water absorption at age 28-day results.

3.2. Water Absorption

Figure 4 illustrates the effect of the fiber type and content on concrete absorption at day 28. The inherent characteristics of SLF and BF as plant fibers with a higher water absorption capacity led to an increase in the water absorption of concrete. The water absorption increased by 2.8% and 3.2% when 1.35% of SLF and BF was used in the concrete mixes with a 0.3 W/B ratio, respectively. However, there was a 6.1% reduction in water absorption when using GF with the same content. Based on these results, the relationship between the water absorption of the natural fibers (SLF and BF) and the concrete absorption is a crucial aspect that influences the overall performance of concrete. Generally, as the percentage of these fibers increased, the water absorption of concrete showed a tendency to rise. This is primarily attributed to the hygroscopic nature of SLF and BF, which could absorb and retain water.

3.3. Compressive Strength

The compressive strength results of non-fiber concrete, sisal fiber concrete (SLFC), banana fiber concrete (BFC), and glass fiber concrete (GFC) specimens at 7 days and 28 days are depicted in Figure 5. The outcomes reveal significant enhancements in the cube compressive strength of SLFC and BFC compared to non-fiber concrete. Moreover, the compressive strength increased with the escalation of the fiber content. For the GFC specimens, greater improvements in the compressive strength for the cases of 0.45% and 0.9% volume fractions of GF were relative to SLFC and BFC specimens with the same fiber content, while the 1.35% volume fraction led to lower compressive strength. The notably superior strengthening mechanism of GFC compared to BFC and SLFC could be attributed to the GF surface being covered by cement hydration products and the robust adhesion between GF and the matrix [26,43].

The control sample (PC-30) registered a compressive strength of 25.11 MPa, slightly exceeding PC-40, which recorded a strength of 25.5 MPa. For the phase I specimens, in comparison to the control sample, the strength at day 7 of SLF-30-135, BF-30-135, and GF-30-135 were the optimal mixes, showing improvements of 9.9%, 11.41%, and 15.23%, respectively. These improvements were 7.5%, 8.77%, and 14.5%, respectively, in the case of a W/B ratio of 0.4. The strengths for the control samples (PC-30 and PC-40) at 28 days were 40.21 MPa and 40.8 MPa for the W/B ratios 0.3 and 0.4, respectively. The improvements for specimens SLF-30-135, BF-30-135, and GF-30-90 were 1.92%, 2.84%, and 3.98%, respectively, in the case of a 0.3 W/B ratio. However, these improvements were 2.80%, 4.36%, and 4.80%, respectively, in the case of a 0.4 W/B ratio. The fibers were uniformly dispersed within the matrix, creating a three-dimensional network structure [14,22]. This structure serves to impede the initiation and spreading of cracks, bridge existing cracks, diminish stress concentration at crack tips, redistribute stress, alter the crack propagation direction, hinder secondary crack expansion, and slow down the overall crack development rate [44,45].

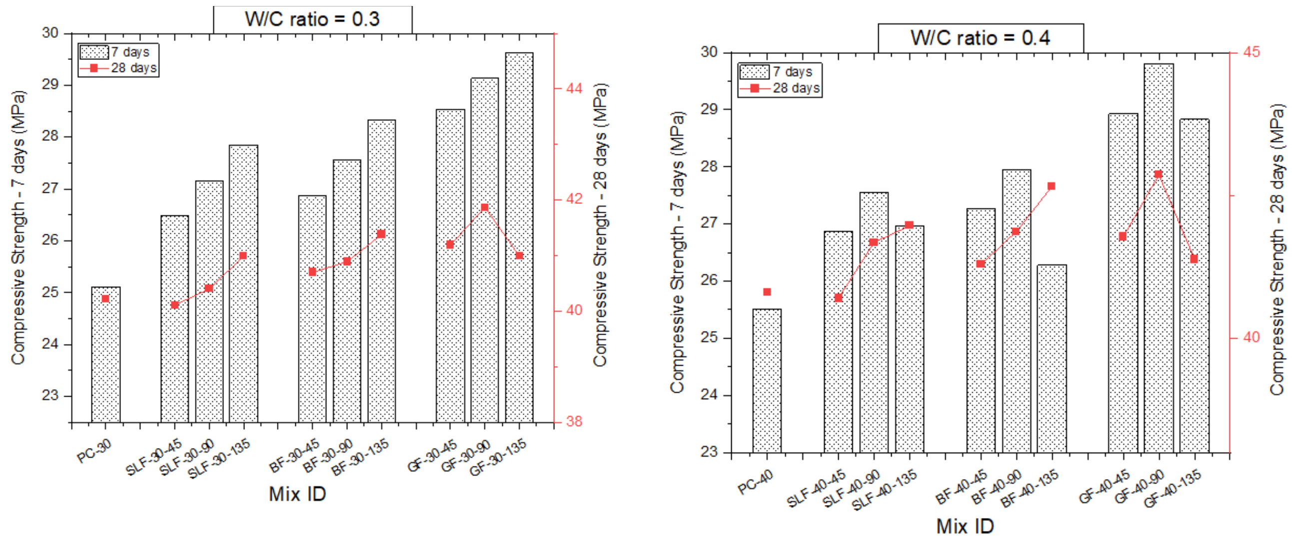

(**a**) For the water/binder ratio of 0.3 (**b**) For the water/binder ratio of 0.4

Figure 5. Effect of the fiber type and content on the concrete compressive strength.

3.4. Splitting Tensile Strength

The records for the non-fiber concrete, SLFC, BFC, and GFC specimens are presented in Figure 6. For the 7-day cube splitting tensile strength, the control sample (PC-30) registered 2.68 MPa, while (PC-40) exhibited 2.95 MPa. In comparison to the control sample, under a W/B ratio of 0.3, the 7-day strength of SLF-30-135, BF-30-135, and GF-30-135 exhibited increases of 6.6%, 9.45%, and 14.31%, respectively. However, under a W/B ratio of 0.4, these increases were 6.00%, 7.27%, and 7.4%, respectively. On the other hand, the 28-day cube splitting tensile strength of SLF-30-135, BF-30-135, and GF-30-135 increased by 6.0%, 7.27%, and 9.10%, respectively, in the case of the W/B ratio of 0.3. Moreover, these improvements were 3.60%, 6.94%, and 10.38%, respectively, in the case of the 0.4W/B ratio.

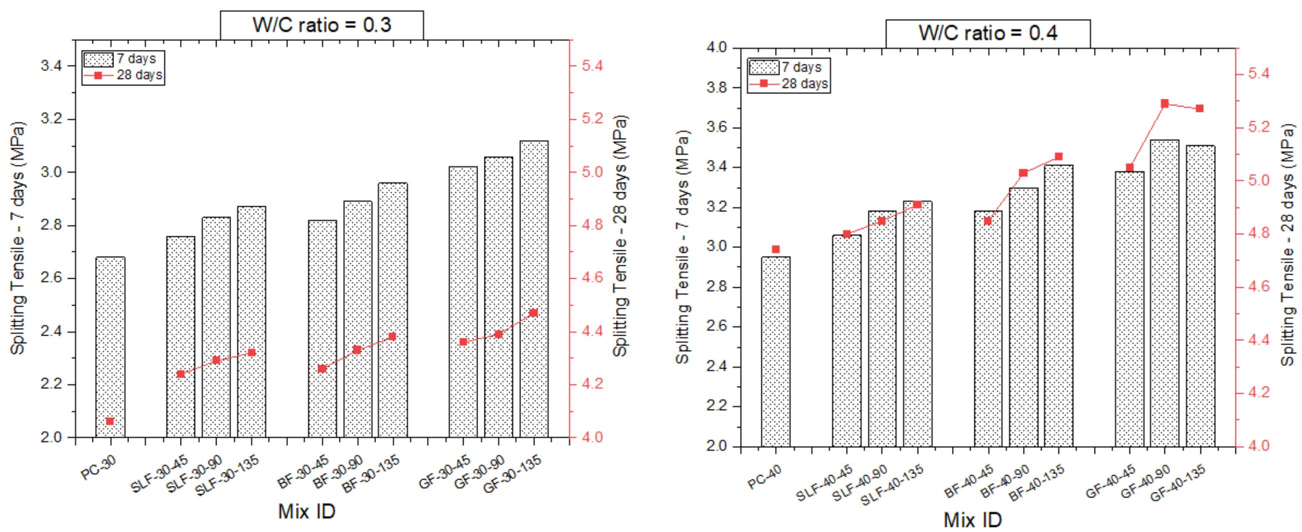

(**a**) For the water/binder ratio of 0.3 (**b**) For the water/binder ratio of 0.4

Figure 6. Effect of the fiber type and content on the concrete tensile strength.

3.5. Flexural Strength

Figure 7 illustrates the results of flexural strength for specimens of non-fiber concrete, SLFC, BFC, and GFC at water-to-binder ratios of 0.30 and 0.4. The addition of fibers, especially GF, resulted in an enhancement of the flexural strength of the concrete up to a volume fraction of 1.35%. For the phase I specimens, the flexural strength of all types of fiber specimens increases with all percentages (%) of fibers for both day 7 and day 28. The maximum values of 3.54 MPa and 5.29 MPa were observed in GF-40-90 at 7 and 28 days, respectively, which were 32.1% and 97.4% higher than that of PC-40 at the same age. For the W/B ratio of 0.4, the flexural strength of the GFC specimens exhibited an initial increase followed by a subsequent decrease with the increase in the GF dosage. The optimal GF dosage was 0.9%, which resulted in a corresponding flexural strength of 5.29 MPa.

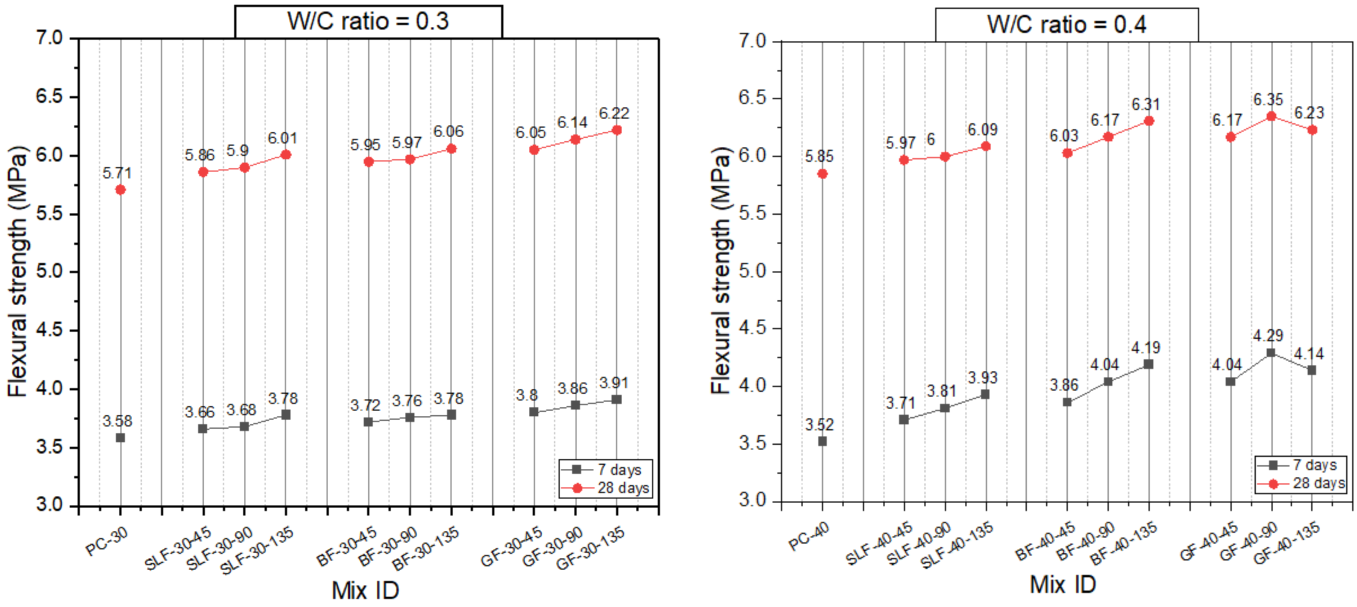

(**a**) For the water/binder ratio of 0.3 (**b**) For the water/binder ratio of 0.4

Figure 7. Effect of the fiber type and content on the concrete flexural strength.

3.6. Micromorphology Analysis

SEM analysis was employed to examine the morphology of the concrete, aiming to elucidate the impact of fibers on the interfacial transition zones (ITZs), microcracks, and their propagation within the matrix connecting the fiber cement paste and aggregate cement paste. Specimens with a diameter ranging from 5 to 10 mm were extracted from cubes subjected to compressive testing. The SEM images of the fiber-free mixture (control samples) are presented in Figure 8. The control mixtures exhibited a porous morphology with varied diameters and a standard setting, and the ITZ was identified between the bulk paste and aggregate composite measuring approximately 45 µm. Furthermore, a positive bond quality was observed between the cement matrix and aggregate, and the cement matrix demonstrated a high degree of compactness. However, it is noteworthy that the cracks in PC-30 were more pronounced than those in PC-40.

The SEM analysis was carried out on the most favorable samples based on the results of the mechanical properties. For the W/B of 0.3, the selected samples were SLF-30-135, BF-30-135, and GF-30-90, while samples SLF-40-135, BF-40-135, and GF-40-90 were selected for the phase II samples. Figure 9 shows a comparison between the SEM images for samples SLF-30-135 and SLF-40-135. The micromorphology of SLF-30-135 revealed a loosely bonded connection between the SLF and the matrix, which contributed to the degradation of the concrete's strength properties. The adhesive strength between the SLF and the cement matrix markedly diminished compared to the control sample, owing to the inherent weaker cohesion between fibers and concrete, as indicated by reference [15]. Nevertheless, the presence of microscopic protrusions, originating from the cement hydration process, led to surface irregularities in the SLF. This unevenness facilitated a tangible interlocking effect at the interfaces, ultimately enhancing the connection between the SLF and the matrix. The interaction between the SLF and concrete was more effective when a W/B ratio of 0.4 was employed compared to its counterpart with a W/B ratio of 0.3. Figure 10 shows a comparison between the SEM images of samples BF-30-135 and BF-40-135. Identical behavior was exhibited in these samples as in those with SLF, in alignment with [33].

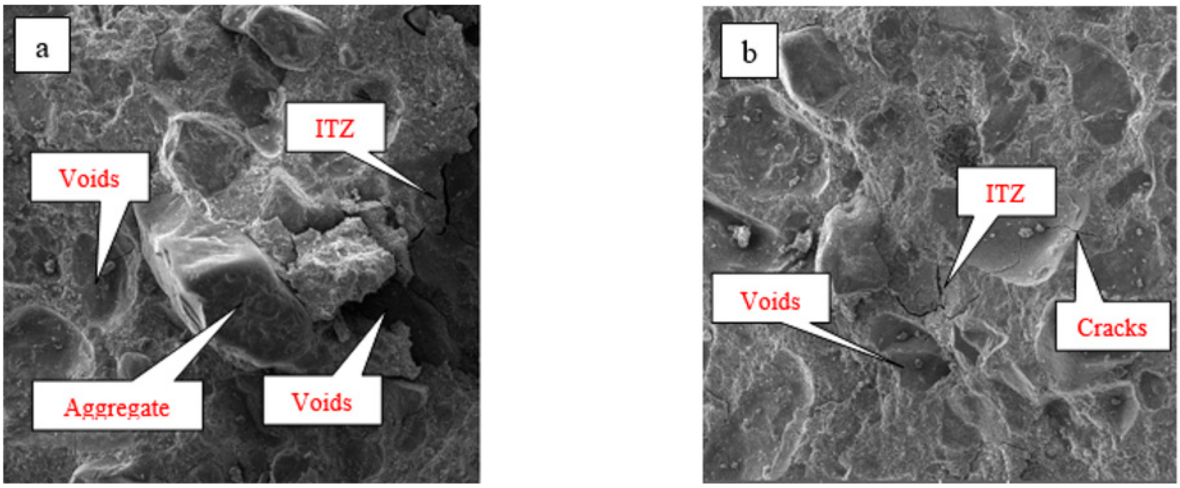

Figure 8. The SEM morphology of the control samples (magnification × 100). (**a**) For the water/binder ratio of 0.3; (**b**) For the water/binder ratio of 0.4.

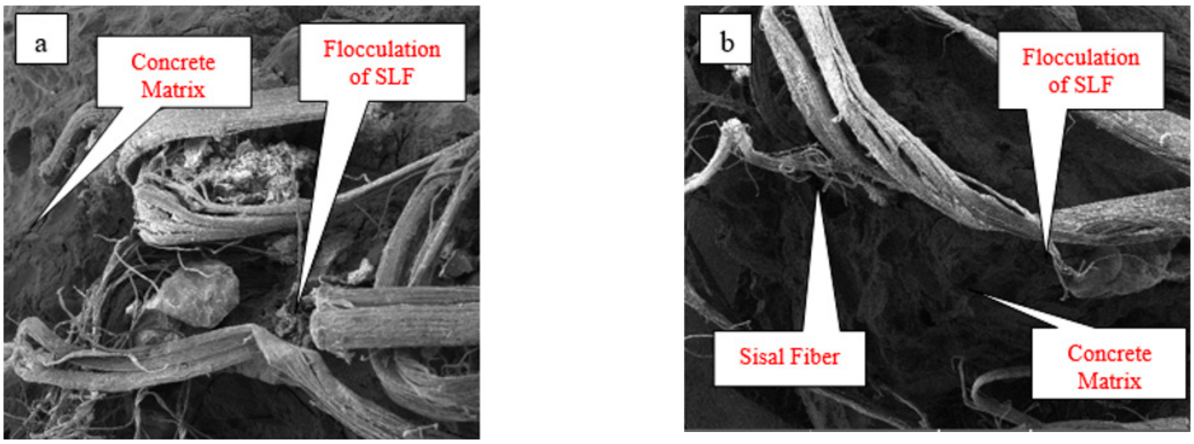

Figure 9. The SEM morphology of the SLF-30-135 sample. (**a**) For the water/binder ratio of 0.3—magnification × 50; (**b**) For the water/binder ratio of 0.4—magnification × 25.

Figure 11 presents a comparison between GF-30-90 and BF-40-90. Despite a GF dosage reaching 0.9%, the adhesive strength between GF and the matrix, as well as between the aggregate and matrix, remained excellent, while the cement matrix of GF-30-90 exhibited numerous pores and voids with relatively uniform pore sizes. Additionally, in the case of GF-30-90, there was a void with a larger size. The macro voids in GF-30-135 were the main factor behind the rapid decline in strength and the ongoing rise in water absorption. Additionally, when the water-to-binder ratio increased to 0.4, the optimum GF content decreased from 1.35% to 0.90%, aligning with findings from prior studies [46].

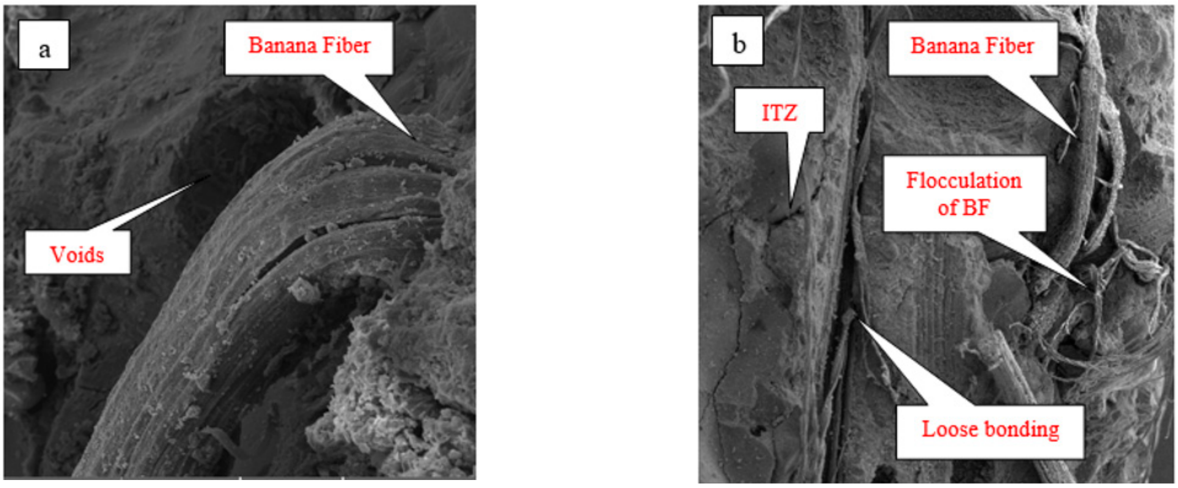

Figure 10. The SEM morphology of the BF-30-135 sample. (**a**) For the water/binder ratio of 0.3—magnification × 300; (**b**) For the water/binder ratio of 0.4—magnification × 50.

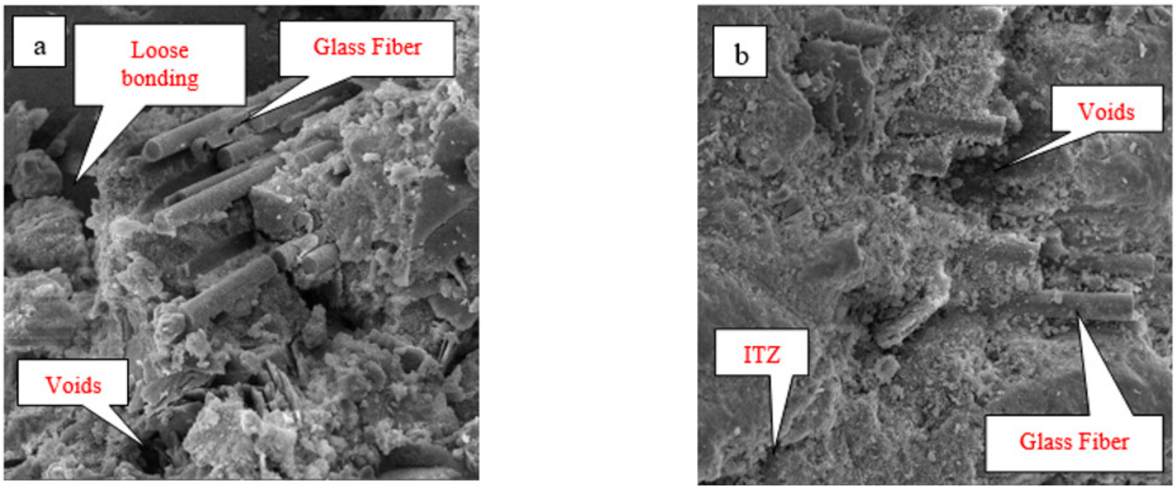

Figure 11. The SEM morphology of GF-30-90 sample. (**a**) For the water/binder ratio of 0.3—magnification × 500; (**b**) For the water/binder ratio of 0.4—magnification × 500.

4. Conclusions

This paper presents the outcomes of an extensive experimental study that explores the impact of SLF, BF, and GF on the mechanical and microstructural properties of concrete. Concrete specimens were prepared using different W/B ratios, fiber contents, and curing times. These specimens were tested to obtain data about the compressive, flexural, and splitting tensile strengths. Moreover, the completed water absorption curves of SLFC, BFC, and GFC were explored. Additionally, SEM observations were carried out to obtain micro-analysis and failure analysis of the tested specimens. From the experimental findings, the following conclusions can be drawn:

1. The reduction in workability was enhanced in the cases of SLF and BF relative to the case of GF. This could be attributed to the water absorption by the SLF and BF. The inherent characteristics of SLF and BF as plant fibers with a higher water absorption capacity led to these reductions in workability.
2. The relationship between the water absorption of SLF and BF and the concrete absorption was a crucial aspect that influenced the overall performance of concrete. As the percentage of these fibers increased, there were rises in the water absorption of concrete.

3. The outcomes revealed significant enhancements in the mechanical properties of SLFC and BFC compared to the non-fiber concrete. Moreover, these properties increased with the escalating of the fiber content. Higher improvements were obtained for the GFC relative to the SLFC and BFC specimens with the same fiber content.
4. The micromorphology of the samples with SLF and BF revealed loosely bonded connections between the fibers and the matrix, which contributed to the degradation of the concrete's strength properties. The adhesive strength between the fibers and the cement matrix was significantly lower than that of the control sample due to the weak cohesive strength between fibers and concrete.

5. Limitations and Future Work

Studying sisal fiber, glass fiber, and banana fiber in concrete presents both limitations and promising prospects. One limitation lies in the variability of fiber characteristics, including length, diameter, and tensile strength, which can affect their performance in concrete. Additionally, the compatibility of these fibers with concrete mixtures and their long-term durability under various environmental conditions are in need of further investigation. By optimizing fiber proportions and concrete mix designs, researchers can enhance the mechanical properties and durability of fiber-reinforced concrete. Moreover, exploring innovative methods for fiber extraction and treatment can improve the uniformity and quality of fibers, leading to more consistent performance in concrete. Furthermore, incorporating advanced analytical techniques, such as microscopy and computational modeling, can provide deeper insights into the behavior of fiber-reinforced concrete, paving the way for the development of sustainable and resilient construction materials.

Author Contributions: Conceptualization, A.A.-K.A.A.S.; Data curation, S.E., A.E.-Z., S.M.M.S. and T.I.S.; Formal analysis, A.E.-Z., A.M.S. and T.I.S.; Investigation, S.M.M.S.; Methodology, S.M.M.S. and A.A.-K.A.A.S.; Resources, W.F.E., S.E. and A.M.S.; Software, W.F.E., S.E., A.E.-Z., A.M.S. and T.I.S.; Supervision, A.A.-K.A.A.S.; Validation, S.M.M.S. and A.A.-K.A.A.S.; Visualization, W.F.E.; Writing—original draft, W.F.E., S.E. and A.M.S.; Writing—review and editing, A.E.-Z. All authors have read and agreed to the published version of the manuscript.

Funding: This research received partially financed by the Kingdom University (2023-11-014).

Data Availability Statement: The data presented in this study are available on request from the corresponding author.

Acknowledgments: The authors would like to acknowledge that this research work was partially financed by Kingdom University, Bahrain from the research grant number 2023-11-014.

Conflicts of Interest: The authors declare no conflicts of interest.

References

1. Thomas, B.C.; Jose, Y.S. Materials Today: Proceedings A study on characteristics of sisal fiber and its performance in fiber reinforced concrete. *Mater. Today Proc.* **2021**, *51*, 1238–1242. [CrossRef]
2. Kabir, R.; Islam, M. Bond stress behavior between concrete and steel rebar: Critical investigation of pull-out test via Finite Element Modeling. *Int. J. Civ. Struct. Eng.* **2014**, *5*, 80–90. [CrossRef]
3. de Klerk, M.D.; Kayondo, M.; Moelich, G.M.; de Villiers, W.I.; Combrinck, R.; Boshoff, W.P. Durability of chemically modified sisal fibre in cement-based composites. *Constr. Build. Mater.* **2020**, *241*, 117835. [CrossRef]
4. De Souza, R.; Maria, L.; De Souza, S.; De Andrade, F. Comparative study on the mechanical behavior and durability of polypropylene and sisal fiber reinforced concretes. *Constr. Build. Mater.* **2019**, *211*, 617–628. [CrossRef]
5. Lima, P.R.L.; Roque, A.B.; Fontes, C.M.A.; Lima, J.M.F.; Barros, J.A.O. Potentialities of cement-based recycled materials reinforced with sisal fibers as a filler component of precast concrete slabs. In *Sustainable and Nonconventional Construction Materials Using Inorganic Bonded Fiber Composites*; Woodhead Publishing: Sawston, Cambridge, 2017; pp. 399–428. [CrossRef]
6. Sabarish, K.V.; Paul, P.; Bhuvaneshwari; Jones, J. An experimental investigation on properties of sisal fiber used in the concrete. *Mater. Today Proc.* **2020**, *22*, 439–443. [CrossRef]
7. Lima, P.R.L.; Barros, J.A.O.; Roque, A.B.; Fontes, C.M.A.; Lima, J.M.F. Short sisal fiber reinforced recycled concrete block for one-way precast concrete slabs. *Constr. Build. Mater.* **2018**, *187*, 620–634. [CrossRef]
8. Jahim, H. The Use Of Wollastonite To Enhance Fresh And Mechanical Properites of Concrete. Ph.D. Thesis, Baghdad University, Baghdad, Iraq, 2010.

9. El-azim, A.; El-Aziz, A.; Hasan, F. Mechanical Behavior of Concrete Containing One Type and Hybrid Fibers. *Egypt. Int. J. Mech. Behav. Concr. Contain. Type Hybrid Fibers* **2018**, *24*, 27–33. [CrossRef]
10. Amezugbe, F.A. The Performance of Natural and Synthetic Fibers in Low Strength Mortar: A Pilot Study of Six Selected Fibers. Ph.D. Thesis, University of Florida, Gainesville, FL, USA, 2013; pp. 1–75.
11. Swathi, V.; Asadi, S.S. An influence of pozzolanic materials with hybrid fibers on structural performance of concrete: A review. *Mater. Today Proc.* **2020**, *43*, 1956–1959. [CrossRef]
12. Padanattil, A.; Jayanarayanan, K.; Mini, K.M. Novel hybrid composites based on glass and sisal fiber for retrofitting of reinforced concrete structures. *Constr. Build. Mater.* **2017**, *133*, 146–153. [CrossRef]
13. Saravanan, R.; Malyadri, T.; Rao, M.S.S.; Sunkara, N. Synthesize and characterization of maleic acid treated banana fiber composites. *Mater. Today Proc.* **2019**, *18*, 5382–5387. [CrossRef]
14. Izquierdo, I.S.; Izquierdo, O.S.; Ramalho, M.A.; Taliercio, A. Sisal fiber reinforced hollow concrete blocks for structural applications: Testing and modeling. *Constr. Build. Mater.* **2017**, *151*, 98–112. [CrossRef]
15. Ren, G.; Yao, B.; Huang, H.; Gao, X. Influence of sisal fibers on the mechanical performance of ultra-high performance concretes. *Constr. Build. Mater.* **2021**, *286*, 122958. [CrossRef]
16. Niyasom, S.; Tangboriboon, N. Development of biomaterial fillers using eggshells, water hyacinth fibers, and banana fibers for green concrete construction. *Constr. Build. Mater.* **2021**, *283*, 122627. [CrossRef]
17. Kumar, S.S.; Akash, B.M.; Kabilan, M.; Karna, H.; Navaneethan, S. An Experimental Study and Behaviour of Banana Fiber in Concrete. *Int. J. Sci. Eng. Res.* **2019**, *10*, 10–14. Available online: http://www.ijser.org (accessed on 20 March 2023).
18. Mostafa, M.; Uddin, N. Experimental analysis of Compressed Earth Block (CEB) with banana fibers resisting flexural and compression forces. *Case Stud. Constr. Mater.* **2016**, *5*, 53–63. [CrossRef]
19. Akinyemi, B.A.; Dai, C. Development of banana fibers and wood bottom ash modified cement mortars. *Constr. Build. Mater.* **2020**, *241*, 118041. [CrossRef]
20. Chandramouli, K.; Pannirselvam, N.; Pardhu, D.V.V.N.S.; Anitha, V. Experimental investigation on banana fibre reinforced concrete with conventional concrete. *Int. J. Recent Technol. Eng.* **2019**, *7*, 874–876.
21. Dhawan, A.; Gupta, N.; Goyal, R.; Saxena, K.K. Evaluation of mechanical properties of concrete manufactured with fly ash, bagasse ash and banana fibre. *Mater. Today Proc.* **2021**, *44*, 17–22. [CrossRef]
22. Naaamandadin, N.A.; Saharudin, A.I.; Mustafa, W.A.; Santiagoo, R. Mechanical behaviour of banana fibre reinforced concrete with kenaf fibre as an additive. In *Lecture Notes in Mechanical Engineering*; Springer: Singapore, 2020; pp. 207–213. [CrossRef]
23. Yue, C.; Hu, X. Tensile properties of short-glass-fiber- and short-carbon-fiber-reinforced polypropylene composites. *Compos. Part A Appl. Sci. Manuf.* **2000**, *31*, 1117–1125.
24. Khan, M.; Ali, M. Use of glass and nylon fibers in concrete for controlling early age micro cracking in bridge decks. *Constr. Build. Mater.* **2016**, *125*, 800–808. [CrossRef]
25. Choi, Y.; Yuan, R.L. Experimental relationship between splitting tensile strength and compressive strength of GFRC and PFRC. *Cem. Concr. Res.* **2005**, *35*, 1587–1591. [CrossRef]
26. Kizilkanat, A.B.; Kabay, N.; Akyüncü, V.; Chowdhury, S.; Akça, A.H. Mechanical properties and fracture behavior of basalt and glass fiber reinforced concrete: An experimental study. *Constr. Build. Mater.* **2015**, *100*, 218–224. [CrossRef]
27. Madhkhan, M.; Katirai, R. Effect of pozzolanic materials on mechanical properties and aging of glass fiber reinforced concrete. *Constr. Build. Mater.* **2019**, *225*, 146–158. [CrossRef]
28. *ES 4756-1*; Cement Part:(1) Composition, Specifications And Conformity Criteria For Common Cements. Egyptian Organization for Standardization and Quality (EOS): Cairo Governorate, Egypt, 2013.
29. *EN 197-1*; Cement—Part 1: Composition, Specifications and Conformity Criteria for Common Cements Ciment. European Committee For Standardisation: London, UK, 1992.
30. Sika ViscoCrete-3425. Available online: https://egy.sika.com/en/construction/concrete-admixture/admixture-types/high-range-waterreducers/sika-viscocrete-3425.html (accessed on 10 April 2022).
31. *ASTM C494/C494M*; Standard Specification for Chemical Admixtures for Concrete. iTeh, Inc.: Newark, DE, USA, 2019. [CrossRef]
32. *ASTM C33/C33M*; Standard Specification for Concrete Aggregates. ASTM International: West Conshohocken, PA, USA,, 2018. [CrossRef]
33. *ASTM D123*; Standard Terminology Relating to Textiles. ASTM International: West Conshohocken, PA, USA, 2019. [CrossRef]
34. Attia, M.M.; Al Sayed, A.A.K.A.; Tayeh, B.A.; Shawky, S.M.M. Banana agriculture waste as eco-friendly material in fibre-reinforced concrete: An experimental study. *Adv. Concr. Constr.* **2022**, *14*, 355–368. [CrossRef]
35. *ACI 211.1-91*; Standard Practice for Selecting Proportions for Normal, Heavyweight, and Mass Concrete. ACI Committee 211; American Concrete Institute: Farmington Hills, MI, USA, 2002.
36. *ACI PRC-544.1R-96*; Report on Fiber Reinforced Concrete. American Concrete Institute: Farmington Hills, MI, USA, 2009.
37. *ASTM C143/C143M*; Standard Test Method for Slump of Hydraulic-Cement Concrete. ASTM International: West Conshohocken, PA, USA, 2015. [CrossRef]
38. *BS 1881-124*; Testing Concrete—Methods for Analysis of Hardened Concrete. British Standards Institution (BSI): London, UK, 2021.
39. *ASTM C78/C78M*; Standard Test Method for Flexural Strength of Concrete. ASTM International: West Conshohocken, PA, USA, 2022. [CrossRef]

40. *ASTM C496/C496M*; Standard Test Method for Splitting Tensile Strength of Cylindrical Concrete Specimens. ASTM International: West Conshohocken, PA, USA, 2011. [CrossRef]
41. *ASTM C642*; Standard Test Method for Density, Absorption, and Voids in Hardened Concrete. ASTM International: West Conshohocken, PA, USA, 2021. [CrossRef]
42. *ASTM C1723*; Standard Guide for Examination of Hardened Concrete Using Scanning Electron Microscopy. iTeh, Inc.: Newark, DE, USA, 2016. [CrossRef]
43. Paktiawal, A.; Alam, M. Alkali-resistant glass fiber high strength concrete and its durability parameters. *Mater. Today Proc.* **2021**, *47*, 4758–4766. [CrossRef]
44. Yuan, Z.; Jia, Y. Mechanical properties and microstructure of glass fiber and polypropylene fiber reinforced concrete: An experimental study. *Constr. Build. Mater.* **2021**, *266*, 121048. [CrossRef]
45. Anand, S.; Varshney, H. An Experimental Evaluation on Effect of Chopped Glass Fiber in Conventional Concrete. *Int. J. Adv. Res. Sci. Eng.* **2018**, *7*, 556–562.
46. Griffiths, R.; Ball, A. An assessment of the properties and degradation behaviour of glass-fibre-reinforced polyester polymer concrete. *Compos. Sci. Technol.* **2000**, *60*, 2747–2753. [CrossRef]